In-Situ Bulk Polymerization of Dilute Particle/MMA Dispersions

Mustafa M. Demir, Patrice Castignolles,† Ümit Akbey, and Gerhard Wegner*

Max Planck Institute for Polymer Research, Ackermannweg 10, D-55128 Mainz, Germany

Received January 18, 2007; Revised Manuscript Received April 2, 2007

ABSTRACT: Composites of poly(methyl methacrylate) and various nanoscale inorganic particles (zinc oxide, titanium dioxide, zirconium dioxide, silicon dioxide, and aluminum nitride) were prepared by in-situ bulk polymerization using 2,2′-azobis(isobutyronitrile) as initiator. The particles of ZnO, TiO_2, and ZrO_2 were surface-modified by alkylphosphonic acids to render them dispersible in the monomer. The effect of these nanoparticles on the free radical polymerization was investigated. Regardless of chemical nature and size, the particles suppress the autoacceleration which would otherwise occur in the bulk free-radical polymerization of methyl methacrylate (MMA). A degenerative chain transfer is proposed to take place between surface-adsorbed water on the particles and propagating chain radicals. This reaction competes with normal termination. Formation of vinylidene chains ends originating from disproportionation is suppressed. In consequence, thermal stability of PMMA produced in the presence of particles is improved. Aggregation of individual particles upon polymerization has been observed and presumably is due to interparticle depletion attraction, even though the particles are individually dispersed in the monomer. Formation of particle clusters is suppressed when a difunctional monomer (e.g., ethylene glycol dimethacrylate) is used as comonomer. The cross-linked medium slows down the diffusion of the particles and therefore interferes with particle aggregation via a depletion mechanism.

Introduction

The combination of inorganic solid particles and polymers is of great interest for numerous existing and potential applications of composite materials in various fields of science and technology.[1−3] The general principle of preparation of these composites involves mechanical mixing of the particles with a prefabricated polymer to obtain a so-called compound which can be processed by further conventional techniques for instance extrusion and injection molding. The particles are frequently surface-modified or compounded in the polymer in presence of surfactants in order to enhance the compatibility of the two unlike materials. The increasing popularity of nanoscaled particles which show so-called quantum size effects in terms of optical and electrical behavior has triggered the question whether such particles can be homogeneously dispersed in polymer matrices, thereby giving novel materials by which the unique properties of the inorganic materials can be brought to useful applications. However, nanoscale particles tend to form aggregates, and it is very difficult, if not impossible in many cases, to create mixtures ("compounds") of a given polymer with the desired particles in which the particles are individually and homogeneously dispersed. The nanoparticles rather aggregate and form "clouds" or clusters as a consequence of depletion forces acting between individual particles in the melt or a solution of linear polymers. This mechanism purely driven by entropic forces occurs also when enthalpic interactions between the particles have been minimized by modification of their surfaces. Polymerization of a mixture of monomer with the desired particles, starting with a suspension of particles in a suitable monomer, seems to be a possibility to overcome the many difficulties encountered in "compounding" prefabricated polymer and particles. This method is known as in-situ bulk polymerization and allows high rate of polymerization and high purity of the polymer. In this work, we report on a comparative case study of the process of in-situ bulk polymerization of dispersions of various nanoparticles in methyl methacrylate (MMA). Moreover, we have examined the stability of the particles against aggregation upon polymerization of initially homogeneous particle/monomer suspension. The results and discussion of this systematic study are presented in two separate sections of this article. In the first section, the effect of particles on the mechanism of free radical bulk polymerization of MMA is reported, demonstrating that the particle surface interacts with the propagating free radicals. The polymerization process is examined in terms of conversion profiles, molecular weight distributions (MWDs) of formed polymer, and thermal stability of the resulting composite materials. In the second section, the dispersion of the particles with the in-situ-formed poly(methyl methacrylate) (PMMA) is presented. The state of aggregation of the particles in PMMA composites was characterized by transmission electron microscopy (TEM) by which the depletion-induced flocculation can be documented. It will also be demonstrated that in-situ cross-linking which hampers diffusion of the particles and PMMA chains is able to suppress flocculation.

The surface of inorganic solids is, generally speaking, energy-rich and chemically reactive and hence is covered with adsorbed water when in contact with moist air.[4,5] In particular, the surface of oxides and nitrides usually absorbs water to form surface hydroxyls, on which further water becomes physisorbed through hydrogen bonding.[6,7] In this article, we use the term "surface hydroxyls" for both OH group on the crystal surface and adsorbed water molecules present on the surface via hydrogen bonding. Nagao et al.[4] reported the occurrence of condensation of water molecules due to the strong lateral interaction between water molecules adsorbed on a homogeneous surface in addition to their interaction with the underlying surface. Nosaka and Nosaka[8] categorized water adsorbed to the surface of TiO_2 powders into four distinctively different species having different dynamics proven by temperature-dependent NMR spectroscopy. Four types of surface-adsorbed water coexist, namely (i) rigid water species with restricted mobility near the solid surface,

* Corresponding author: Tel +49 6131 379 130; Fax +49 6131 379 330; e-mail wegner@mpip-mainz.mpg.de.

† Current address: Key Centre for Polymer Colloids, School of Chemistry F11, University of Sydney, NSW 2006, Australia.

10.1021/ma070142e CCC: $37.00
Published on Web 05/09/2007

(ii) less mobile water molecules in the intermediate water layer, (iii) relatively mobile water molecules in the outer water layer, and (iv) very loosely adsorbed water which exchange slowly with gaseous water in the air. Amorphous silica, which is commonly used as drying agent, may be among the richest particles in terms of the chemistry of surface hydroxyl groups.[9] In addition to oxides, AlN is also sensitive to atmospheric moisture and interacts with water in a hydrolysis reaction to decompose into aluminum hydroxide.[7]

The species located at the surface (hydroxyl groups, water molecules, oxygen, etc.) are active and have important consequences in catalysis,[10] photocatalysis, surface modification,[11,12] surface-initiated polymerization,[13,14] etc. For example, Advincula[15] in a recent review summarizes the surface-initiated polymerization radially outward from various particle surfaces where the initiator was chemically grafted to the particle surface via surface hydroxyl groups. Recently, Zhu et al.[16] showed that the presence of water on the surface of ZrO_2 stabilizes surface-adsorbed formaldehyde against nucleophilic attack of oxygen in the surface planes. Semiconductor particles like ZnO[17] and TiO_2[18] have been used as initiators or sensitizers in UV photopolymerization. In the case presented here, the surface groups may interfere with the mechanism of free radical polymerization which—as we will demonstrate—gives a better control on the properties of the polymer matrix in the composite materials.

In colloidal science it is known since long that the addition of macromolecules to a colloidal suspension in a low molecular weight solvent induces an interparticle "depletion" attraction. The range and depth of depletion are functions of the molecular weight and concentration of the polymer.[19] Even at low polymer concentrations (e.g., 1 wt %), the depletion attraction can be strong enough to introduce flocculation of particles.[20] In an in-situ free radical polymerization, the concentration of polymer increases proportional to conversion. The depletion attraction becomes stronger by the formation of new polymer chains and triggers the segregation of particles in the course of polymerization. Considering that depletion needs diffusive motion of both particles and chains, one may expect that the stability of a particle dispersion in the polymer matrix should be enhanced by copolymerization with a difunctional comonomer. The addition of a trace amount of ethylene glycol dimethacrylate (EDMA) to MMA should form a three-dimensional network which could prevent the diffusion and therefore undesirable segregation of the particles.

Experimental Section

Materials. Titanium(IV) oxide (99%), aluminum nitride, and silicon dioxide (Aerosil 300) were commercial nanopowders provided from Sigma, Aldrich, and Degussa, respectively. Zirconium dioxide particles were prepared in the group of Prof. M. Veith of the Leibniz-Institute for New Materials at Saarbrücken/Germany (INM) using sol−gel chemistry as described in the literature.[21] Zinc oxide nanoparticles the surface of which was covered with *tert*-butylphosphonic acid (t-$BuPO_3H_2$) were prepared as described elsewhere.[22,23] Methyl methacrylate (MMA) and 2,2′-azobis(isobutyronitrile) (AIBN) were used as in ref 24. Ethylene glycol dimethacrylate (EDMA) was obtained from Sigma and used without further purification. Absolute ethanol and octylphosphonic acid (99%) (n-OctylPO_3H_2) were obtained Alfa-Aesar.

Nanoparticle Synthesis and Surface Modification. SiO_2 and AlN could be dispersed in the monomer without further surface modification. ZnO nanoparticles had been synthesized with a hydrophobic coating of t-$BuPO_3H_2$ in a one-pot reaction.[23] TiO_2 and ZrO_2 as obtained had a hydrophilic surface. The surface of these nanoparticles was hydrophobized by treatment with n-OctylPO_3H_2 at room temperature. In a typical procedure of surface modification, 200 mg of the desired powder was dispersed in 25 mL of absolute ethanol. The suspension was sonicated for 45 min, and then a solution of 150 mg of n-OctylPO_3H_2 dissolved in 5 mL of absolute ethanol was added to the suspension drop by drop under stirring. The suspension was agitated for further 24 h at ambient conditions to achieve homogeneous coverage by the alkylphosphonic acid. The modified particles were centrifuged at 4000 rpm, washed with absolute ethanol to remove unreacted surfactant, and dried in vacuo at 50 °C.

Table 1. Nanoparticles Used in the Bulk Polymerization of MMA

powder	supplier	surfactant, type and coverage/μmol m^{-2}		mean particle diam/nm[a]	fwhm of PSD[b]
ZnO	MPI-P	t-$BuPO_3H_2$	2.5	22	18
ZrO_2	INM	n-OctylPO_3H_2	2.3	50	57
SiO_2	Degussa			22	23
TiO_2	Sigma	n-OctylPO_3H_2	1.8	400	296
AlN	Aldrich			400	323

[a] Determined by DLS of the dispersion in bulk MMA. [b] Full width at half-maximum of particle size distribution (PSD) obtained from DLS.

Preparation of PMMA/Particle Nanocomposites. The particles were dispersed into MMA. The weight fraction of particles was kept constant at 0.06 (120 mg particle in 2 mL of MMA). The dispersions were sonicated for 20 min and kept overnight to achieve complete wetting of the particle surface. After a second ultrasonication for 30 min, AIBN (1.5 wt %) was added, and three cycles of a freeze−thaw process were applied prior to polymerization. Polymerization was carried out at 60 °C using AIBN as initiator. The glass tubes containing the MMA/particle mixture were placed into a preheated bath at 60 °C; the polymerization was performed under vacuum, and it was stopped after the desired time by quenching to room temperature. To obtain a long-chain-branched or cross-linked copolymer, EDMA (5 μL) was added to the dispersion of the particles in MMA prior to polymerization. Copolymerization was achieved as already described above for bulk polymerization of MMA.

Characterization. ^{1}H NMR, size exclusion chromatography, differential scanning calorimetry (DSC), thermogravimetry (TGA), and transmission electron microscopy (TEM) were performed as reported in ref 24. The size of the particles dispersed in MMA was determined by dynamic light scattering (DLS) using a Malvern Zetasizer 3000. Diffuse reflection infrared Fourier transform (DRIFT) spectra were obtained from the particles dispersed in KBr (5 mg:150 mg) using a Nicolet 730 spectrometer in the range of 4000−400 cm^{-1}. ^{1}H solid-state NMR spectra were obtained with a Bruker DRX700 spectrometer operating at 700 MHz equipped with a commercially available variable temperature 2.5 mm MAS spinning probe. The size of the particle clusters was obtained from statistical treatment of TEM images by measuring the cross sections of typically not less than 100 test clusters with help of the software image J.[25] For clusters those were not spherical in shape, the major and minor distances, d_1 and d_2, respectively, were measured for each cluster, and the diameter d was evaluated according to $d = [d_1 d_2]^{1/2}$. Small-angle X-ray scattering (SAXS) of the composite films was performed by a 2-D detector (Highstar, Bruker). The beam energy was 30 kV × 10 mA generated by monochromatized Cu Kα radiation ($\lambda = 1.54$ Å). SAXS intensity was recorded as a function of scattering vector, $q = (4\pi/\lambda)\sin(2\theta)$, where 2θ is the scattering angle. The detectable q range was from $q = 0.8$ to 8.1 Å^{-1} ($\theta = 0.1°-1.7°$). An illumination time of 5 h and a film thickness of 1 mm were kept constant to achieve accurate comparison of scattering intensities.

Results and Discussion

Table 1 gives a survey of the various types of nanoparticles having different chemical nature, surface composition, and size which were incorporated into PMMA by in-situ bulk polymerization. The particles were dispersed in the monomer; the ones

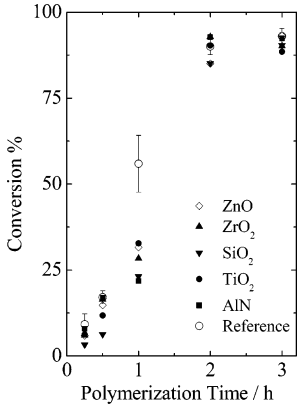

Figure 1. Conversion of MMA at different reaction times in the absence and presence of different types of inorganic particles. The weight fraction of particles is 0.06.

that were not dispersible as obtained from the supplier, for example TiO_2 and ZrO_2, were first hydrophobized ex-situ by treatment with *n*-OctylPO_3H_2 prior to dispersion. SiO_2 and AlN nanopowders were dispersible in MMA as obtained. ZnO nanoparticles hydrophobized with *t*BuPO_3H_2 were prepared in our laboratory as described earlier.[23] The fraction of the total surface of the particles occupied by alkylphosphonic acids was ca. 50%. The hydrophobic surface modification renders the particles compatible with MMA and thereby retards strongly the sedimentation of the particles.

The weight fraction of particles was kept constant at 0.06 with respect to MMA for all particle/MMA systems. This fraction was threshold for particular case of ZnO particles where the suppression of gel effect was observed.[24] For higher fractions, interparticle distance becomes shorter than the size of a polymer chain; thereby strong depletion and eventually segregation are observed in the beginning of polymerization. Moreover, high particle concentrations cause sedimentation that deteriorates the homogeneity of polymerization. The weight fraction we have used was convenient to study both the effect of particles on the polymerization and the level of aggregation without having undesirable sedimentation and severe segregation. The polymerization was carried out in the presence of these particles using AIBN as thermal initiator at 60 °C.

1. In-Situ Polymerization. The polymerization rate and molecular weight distribution of the polymer formed in absence and presence of the particles were examined keeping all parameters constant. The presence of particles markedly influences the free radical polymerization of MMA. Figure 1 shows the conversion to polymer as a function of polymerization time. Conversion was determined by ^{1}H NMR spectroscopy comparing the intensity of monomer signals with those of the polymer. In the reference sample (MMA without particles), a sigmoidal increase of conversion was observed as a function of polymerization time, completely in agreement with literature.[26] The rate of polymerization is similar in both the absence and presence of particles at low conversions. However, the reference sample exhibits a remarkable increase in the rate of polymerization at intermediate conversions. This rapid increase is due to the well-known autoacceleration of polymerization, also known as the gel or Trommsdorf−Norrish effect.[27] Autoacceleration is observed in bulk free radical polymerization of many vinyl monomers, and it originates from the fact that termination is a diffusion-controlled reaction.[28] Because of conversion of monomer to polymer, the viscosity of the medium increases, and this leads to a decrease of the rate of termination, and thus an increase of the concentration of propagating radicals, and

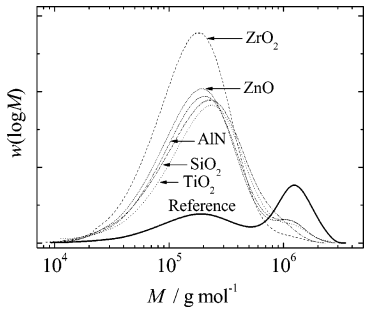

Figure 2. Molecular weight distributions of PMMA after 30 min polymerization time (the samples shown in Figure 1) in the presence of various nanoparticles and for the reference.

thus autoacceleration takes place. However, in the presence of these particles, for instance at 1 h polymerization time, the degree of conversion values appears to be lower compared to that of the reference sample regardless of the size and chemistry of the particles. The particles that have been dispersed into the neat monomer suppress the undesirable autoacceleration. At later stages, the polymerization shows a similar behavior for both reference sample and polymer/particle systems. The polymerization slows down toward a conversion of more than 90% where the propagation becomes diffusion-controlled, and eventually almost complete conversion is achieved all cases. The particles influence not only the shape of the conversion−time curve but also the MWDs of the polymer. Figure 2 presents normalized MWDs of PMMA obtained at 30 min of polymerization time when the onset of autoacceleration emerges in Figure 1. The MWD of the reference sample is found to be bimodal. Two populations of polymer chains are apparent with average molecular weight of 2×10^5 and at 8×10^5. The appearance for this second population with pronouncedly higher molecular weight is a classical signature of the autoacceleration.[26] The reason for this second population is still a question open to debate (local exothermy, propagation by incorporation of macromomonomer as is obtained by disproportionation). While the first population remains at nearly the same MWD, the second population shows a remarkable decrease in the presence of particles. This result can be considered as another evidence of the suppression of the autoacceleration by the nanoscale particles. It is necessary to emphasize that according to common knowledge the appearance of the autoacceleration is dependent on the shape and volume of the reactor in which the polymerization is carried out. These parameters were also kept constant in all the sets of experiments described in Figures 1 and 2.

The observed phenomenon might be a consequence of specific interactions between the particle surface and the propagating free radicals. However, the results seem to be largely independent of the size and chemical nature of the particles. Similar results are observed for both naked and surface-modified particles by phosphonic acid surfactants. These arguments hint that the interaction is specific with regards to the surface group(s) which is (are) common for all the particles. The interaction may lead to the formation of relatively stable intermediate radicals by a transfer reaction which are still active enough to slowly reinitiate the polymerization and eventually lead to an almost complete conversion (the half-life of AIBN in MMA at 60 °C is 16 min,[29] which is too short to ensure a significant radical flux after 2 h). Surface-adsorbed water and oxygen are the first suspects which are common surface species of all oxides and nitrides.

Water is capable to react with surfaces (chemisorption) and shows long-range order phenomena (physisorption) on solid

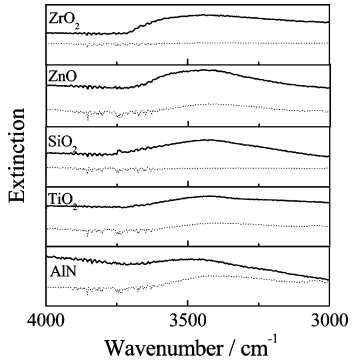

Figure 3. DRIFT analysis of the particles used in the polymerization before (solid lines) and after (dotted lines) annealing at 750 °C for 14 h under nitrogen.

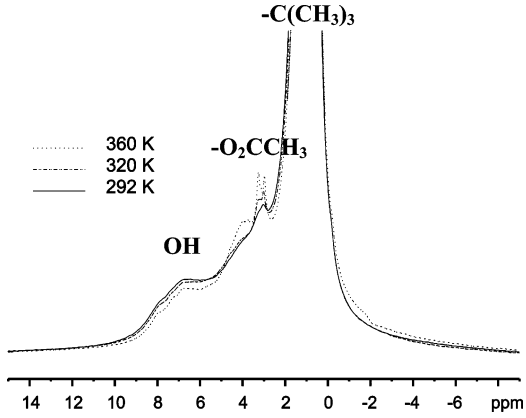

Figure 4. ^{1}H MAS NMR of the ZnO particles at 20, 47, and 87 °C. Thermal desorption of water by increasing temperature from the particle surface is presented.

surfaces.[8] The properties of surface-adsorbed species have been intensively investigated by a number of spectroscopic techniques.[30] The existence of surface hydroxyls and surface-bound water in our samples was confirmed by vibrational and NMR spectroscopy techniques. Annealing experiments at high temperature were performed to remove the chemi- and/or physisorbed water from the particle surface. Diffuse reflection infrared Fourier transform (DRIFT) spectra of the particles before (solid lines) and after annealing at 750 °C for 14 h under nitrogen (dotted lines) are shown in Figure 3. For the ease of comparison, only the part of the spectra between 3000 and 4000 cm^{-1} where the OH band appears is shown. Particles kept under ambient conditions and atmosphere present a broad band centered at around 3500 cm^{-1} which is attributed to surface hydroxyls and/or surface-adsorbed water. After annealing, the band disappears either completely as in the case of ZrO_2 and SiO_2 or partially for the powders of ZnO and TiO_2. The diminishing of the band indicates the presence of sorbed water on the particle surface. AlN is stable to very high temperatures in inert atmosphere. Since the annealing is performed under nitrogen, the annealing process results in fact in a nitridation for this material. The defect sites on the surface of the crystalline nitride become saturated, and thereby the signal of the surface hydroxyls appears to be enhanced.

Controlled heating of the particles in the dark, which exactly stimulates the polymerization conditions, leads to desorption of surface groups including water and oxygen beginning at temperatures above 50 °C.[8,31] Figure 4 presents the fast ^{1}H MAS NMR spectra of the ZnO particles (zincite particles covered by tBuPO$_3$H$_2$) at 20, 47, and 87 °C. The spectra exhibit a broad resonance at ~7 ppm, assigned to the protons of the surface hydroxyl groups. The particles also display very a intense aliphatic resonance at ~1 ppm of the tertiary butyl groups and a relatively weak signal at ~3 ppm due to the methyl groups of acetate species remaining at the surface from the starting material (zinc acetate) of the ZnO synthesis. The spectra have been normalized with respect to the most intense peak, namely the one appearing at 1 ppm in order to compare the intensity of the OH water signal of samples treated at different temperatures. The intensity of the signal of surface hydroxyls gradually decreases in consequences of annealing to about 14% of its initial value as volatile water vaporizes from the particle surface. However, the signal of acetate groups which unlike water are firmly linked to the particle surface becomes narrower due to increase of their mobility. The signals of bidentate and unidentate surface complexes of the acetate moiety appears to be resolved at high 87 °C. The disappearance of the water signal with temperature while the signal of acetate becomes more intense can be attributed to removal of surface water by increasing the temperature of annealing.

Thermal Stability of the Composites. When a vinyl polymer is synthesized via free radical mechanism, chain growth is limited by either termination and/or by transfer reactions. Free radicals terminate through two reactions: disproportionation and combination. The former one results in polymer chains, half of which have a saturated end group and the other half exhibits an unsaturated end group. Termination by combination produces a single head-to-head linkage within one chain. These abnormal residues (unsaturated end group or head-to-head linkage) have a significant influence on the thermal stability of the free radically polymerized polymer.[32,33] For example, growing radicals in MMA polymerization undergo termination mainly by disproportionation (79% at 60 °C) which results in unsaturated vinylidene end groups.[34] PMMA chains having these abnormal linkages are thermally less stable than those with saturated end groups and head-to-tail linkages.[35] In order to evaluate the effect of the presence of particles during polymerization on the thermal stability of the polymer formed, we have examined the thermal degradation of PMMA (Figure 5a). Independent of the nature of the particles, PMMA produced in situ in the presence of these particles turned out to be thermally more stable than the reference sample (solid line) prepared in the absence of particles. While the mass loss in TGA of reference sample is 37% at 300 °C, PMMA obtained in the presence of AlN and ZnO shows a mass loss of only 15% and 7% at this temperature. The differential thermogravimety (DTG) is also presented in Figure 5b. Consistent with previous data in literature,[33,36] PMMA exhibits three degradation steps under nitrogen at a heating rate of 10 °C/min. It starts to degrade by initiation at the head-to-head linkages at around 160 °C, initiation at the unsaturated ends at ~280 °C, and random initiation along the polymer backbone at 370 °C. The contribution of head-to-head linkages to mass loss is relatively small, and it appears as a shoulder of the second peak caused by end-group initiation. The second peak is significantly more intense due to presence of higher number of unsaturated ends (79% disproportionation) than the first one relating to presence of head-to-head linkages (21% combination). However, for the PMMA prepared in the presence of particles, DTG exhibits a single degradation peak that reflects the random scission. The degradation remains only traces of the degradation events which dominate the picture for PMMA prepared under conventional conditions, namely without particles. Kashiwagi et al.[33] reported that chain-transfer agents used in the polymerization process significantly reduce the number of head-to-head linkages and

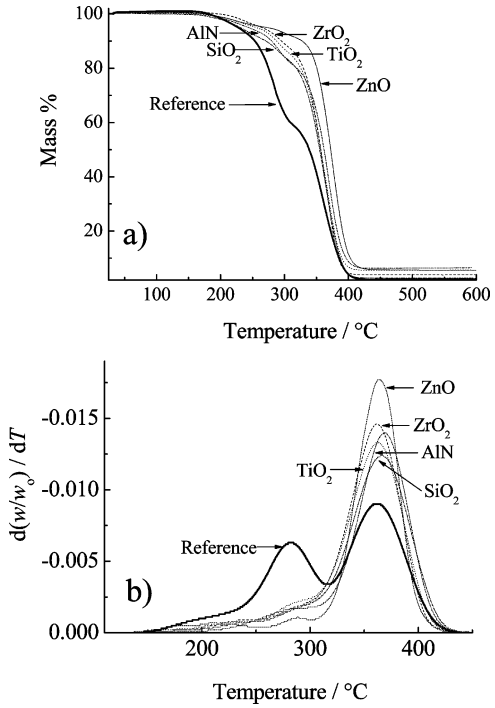

Figure 5. (a) TGA demonstrating patterns of thermal decomposition of pure PMMA (solid line) and its composites with the various particles (dotted lines). (b) Differential TGA traces.

vinylidene ends and thereby stabilize the radically polymerized PMMA. Chain transfer generally consists of the stoppage of the propagation of one chain by hydrogen abstraction from a transfer agent and initiation of a new chain by the radical moiety originated by the abstraction. The disappearance of the second peak in DTG of in-situ polymerized PMMA may indicate a transfer reaction taking place between the particle surface and the propagating free radical in the course of polymerization. This transfer reaction competes with the disproportionation and therefore delays the degradation to the temperature where random scission occurs. It is noteworthy to underline that the composite prepared by simple blending of already formed polymer and particles exhibits the similar thermal degradation profile to that of the reference sample. Therefore, the improvement of the thermal stability of in-situ polymerized PMMA is the result of interaction between propagating chain radicals and the particle surface.

In principle, the transfer reaction we propose should be valid for all vinyl monomers. However, we guess that this reaction is particularly important for vinyl monomers that are terminated by disproportionation like MMA. Since the mechanisms of both the transfer reaction and disproportionation are based on hydrogen abstraction, the former reaction competes with termination using surface-adsorbed water as hydrogen reservoir. In the case of vinyl monomers terminated mainly by combination, for example styrene, the effect of the transfer reaction would not be as dominant as in the case of MMA.

Mechanism of Polymerization. The results reported so far indicate that some species on the particles surfaces react with the propagating PMMA radicals. The particles could induce retardation or inhibition. However, the shape of conversion curves as displayed in Figure 1 shows no retardation and high conversions are achieved within the same polymerization time in both the absence and presence of particles. Therefore, retardation or inhibition can be ruled out. Some moieties on the particles surface could terminate with the propagating radicals either by combination or by disproportionation. Combination should lead to chemical grafting of the propagating PMMA chains to the particle surface. However, the particles before and after polymerization exhibit the same size distributions if dispersed in an organic medium, which rules out the combination. This argument is demonstrated by Figure 6 which shows the size distributions of two representative particles before and after the polymerization. For the latter case the bulk polymerized sample was dissolved and subjected to DLS measurements. The disproportionation inevitably forms vinylidene chain ends that would be detected in thermogravimetric analysis. However, the mass loss originating from the vinylidene end groups is dramatically but not completely suppressed for the PMMA prepared in the presence of particles which rules this hypothesis out. A transfer reaction seems the most plausible interaction taking place between the particles and propagating radicals. It is well-known that classical transfer agents shift the MWDs to smaller average chain lengths, which is not observed at all in our experiments and is demonstrated by Figure 2. A degenerative transfer has thus to take place: the propagating radicals react with the transfer agent leading to a dead polymer chain and a stable radical, which is slow to reinitiate. Hence, the mechanism of the polymerization may contain two competitive chain-stoppage events: conventional termination and degenerative transfer from the particles surface as described by the following kinetic equations:

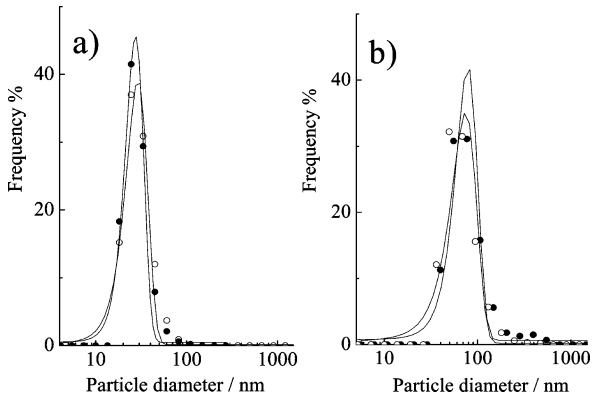

Figure 6. Histograms of diameters representative (a) ZnO and (b) ZrO_2 nanoparticle samples before (hollow circles) and after polymerization (full circles) as determined by DLS in MMA (see text).

termination:

$$\text{disproportionation:}\quad M_n^{\bullet} + M_m^{\bullet} \rightarrow D_n + D_m \qquad k_{t,d}(n,m) \tag{1}$$

$$\text{combination:}\quad M_n^{\bullet} + M_m^{\bullet} \rightarrow D_{n+m} \qquad k_{t,c}(n,m) \tag{2}$$

degenerative transfer reaction:

$$\text{chain stoppage:}\quad M_n^{\bullet} + S \rightarrow D_n + S^* \qquad k_{tr,S} \tag{3}$$

$$\text{reinitiation:}\quad S^* + M \rightarrow M_1^{\bullet} \qquad k_{rei}\ (k_{rei} \ll k_p) \tag{4}$$

where M is the monomer, $M_n^{\bullet}$ is a polymer chain of length n bearing a propagating radical, D_n is the dead polymer of chain length n, and S is the transfer agent situated at the particle surface. Note that this degenerative transfer is not reversible and thus will not induce any control/livingness for the polymerization contrary to what can be obtained for example with RAFT.

At low conversion, the rate coefficient of termination is high and the chain stoppage is mainly by disproportionation. At intermediate conversion, the viscosity of the medium increases

and then the average termination rate coefficient decreases. The reaction with the transfer agent becomes kinetically favored. The chain stoppage moves toward a transfer-controlled regime.[37] The transfer reaction suppresses the autoacceleration by keeping the radical concentration low enough either directly because of slow reinitiation or indirectly by maintaining the rate of termination high enough. Indeed, the transfer reaction must ensure the steady production of small and reactive monomer radicals that maintain the rate of termination at a value high enough to avoid autoacceleration, while most of the chains are stopped by transfer, ensuring that formation of undesired end groups which would affect the thermal stability of the polymer is avoided.

The transfer could take place either in the bulk with molecules having desorbed or on the surface. Reactions in the bulk would consist in a degenerative transfer to water or oxygen. Water was proved not to act as transfer agent in MMA polymerization.[38,39]However, oxygen is very reactive toward alky radicals, and rate coefficients between 5×10^8 and 5×10^9 L mol^{-1} s^{-1} have been reported.[40,41] For the specific case of the polymerization of MMA a rate coefficient 33 000 times higher than the propagation rate coefficient for MMA has been pointed out.[42] Besides, inhibition with oxygen can also cause retardation.[43] The peroxides formed by the reaction with oxygen do not quantitatively reinitiate MMA polymerization under the conditions selected for our experiments.[40] The degenerative transfer thus does not seem plausible to happen in the bulk, but it may take place at the surface of the particles unfortunately, and to the best of our knowledge nothing is known so far in the literature about the reactivity of chemisorbed water or oxygen toward alkyl radicals.

Nanoscale particles provide a large surface area to volume ratio which promotes interfacial reactions. For example, the surface area of our ZnO particles at 6 wt % is 2.9 m^2 mL^{-1} of monomer. Assuming in first approximation a spherical shape for the particles and a uniform size distribution and dispersion, the surface-to-surface interparticle distance (D_s) in the monomer scales with $r(\phi^{-1/3} - 2)$, where r is the radius and ϕ is the volume fraction of the particles. The value of D_s is then 60 nm at 6 wt % for the MMA/ZnO dispersion. Although the distance between the surfaces of two neighboring particles seems large enough for several chains to be initiated and grown in the interstices without touching to the particle surface, the random interaction of every chain with particle surfaces is very likely. A polymer chain that is initiated in the middle between two particles can diffuse to the particle surface. The time required for diffusion is estimated to be on the order of milliseconds, taking the diffusion constant of PMMA ($M_n \sim 10^6$) as 10^{-7} cm^2 s^{-1}.[44,45] Considering the time period of the appearance of the gel effect as 1 h and the entire polymerization of 3 h, collusions between the particle surface and propagating free radicals within this time period must have a high frequency.

2. Level of Aggregation of Particles in Polymer. The macroscopic performance of such composite materials strongly depends on the organization of the nanoscopic solid particles and flexible polymer chains.[1] In systems where the particle surface is protected with hydrophobic material and the chemical interaction between matrix and particles is minimum, particles prefer to form loosely bound aggregates/segregates ("clouds").[23] The presence of nonadsorbing polymer in a homogeneous suspension induces an effective attraction between colloidal particles via the "depletion" mechanism. Exclusion of polymer between two nearby particles gives rise to an unbalanced osmotic pressure which pushes them together. This pressure results in an attractive force which can be described by a depletion potential.[46] In an in-situ polymerization, the medium is dynamic in that it quickly turns from neat monomer into a polymer/monomer mixture and finally to only polymer. In a conventional free radical polymerization, the lifetime of the propagating radicals is very short compared to the time necessary to convert all the monomer so that, once a chain starts, it reacts very rapidly and probably completes its growth in a fraction of a second. Since the number of chains increases with conversion, the interparticle attraction mediated by depletion effect of free polymers becomes favored. Thus, the formation of polymer chains in the homogeneous colloidal suspension perturbs the stability of the particle dispersion in the course of polymerization. Clouds of particles are formed. This phenomenon is observed clearly for the case of ZnO and SiO_2 particles. They give dispersions in MMA for which DLS gives a size of the particles identical to the nonaggregated state (see Table 1). However, they undergo segregation upon polymerization. Figure 7 shows thin section TEM images of PMMA/particle composites of (a) SiO_2, (b) ZrO_2, (c) TiO_2, and (d) AlN and Figure 8a for ZnO. The images present domains or clouds which are rich in terms of particles and a particle-depleted matrix in between the clouds.

In-situ-formed polymer chains are linear and, in fact, form a sufficiently fluid environment such that an individual particle is allowed to diffuse toward other identical particles. The molecular weight and architecture (branching, cross-linking) of polymer are important variables in determining the final size of the particle aggregates in the polymer/particle composites.[47,48] The dispersion of ZnO nanoparticles in both linear and cross-linked PMMA polymerized in situ has been chosen to exemplify this point. Figure 8 shows TEM images of PMMA/ZnO composites obtained under conditions where PMMA of low degree of polymerization (Figure 8a), high degree of polymerization (Figure 8b), and high degree of polymerization additionally cross-linked were formed. The concentration of the initiator in sample of Figure 8a was divided by a factor of 4 to double the number-average length of PMMA chains in Figure 8b assuming the ideal kinetics. The increase in molecular weight has been validated by SEC. The aggregates presented in the electron micrographs (Figure 8a) consist of approximately 4−6 loosely associated individual particles. The hydrodynamic radius of polymer was measured. A value of 5 nm was obtained which is considerably smaller than the particle size. However, the miscibility is promoted when R_g of the linear polymer is larger than the nanoparticle radius as Mackay et al. underlined for a system composed of dendritic polyethylene nanoparticles and linear polystyrene.[48] Increasing the viscosity of the medium by increasing degree of polymerization did not cause a remarkable change of the level of particle dispersion in the linear polymer matrix. Figure 8a,b exhibits an almost identical size of the clouds of inorganic particles, and they contain a similar number of individual particles. Hence, changing the molecular weight of the polymer matrix on this level seems to have no significant effect.

A trace amount of EDMA permits branching and cross-linking of the chains being formed. An abrupt transition from the liquid state to the gel state has been observed when this divinyl monomer was copolymerized with MMA.[49] The presence of EDMA does not qualitatively alter the conversion profile against time.[50] It leads to the appearance of the autoacceleration at lower conversion and polymerization time, whereas the addition of a chain-transfer agent to this system has the opposite effect. In this work, a small quantity of difunctional monomer

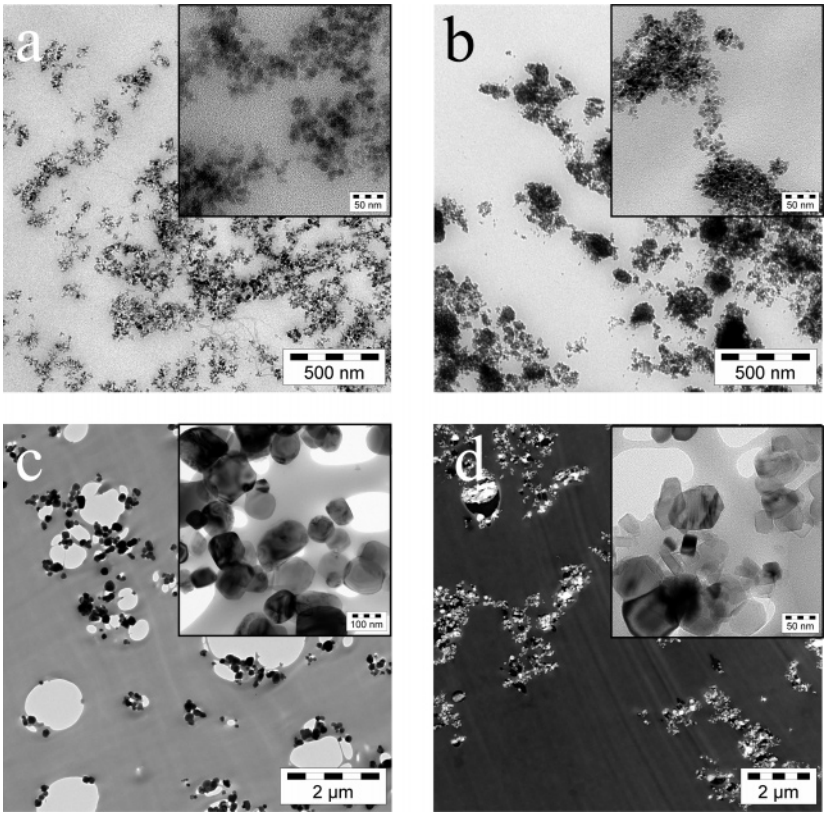

Figure 7. Thin section overview TEM images of the PMMA/particle composites (a) SiO_2, (b) ZrO_2, (c) TiO_2, and (d) AlN.

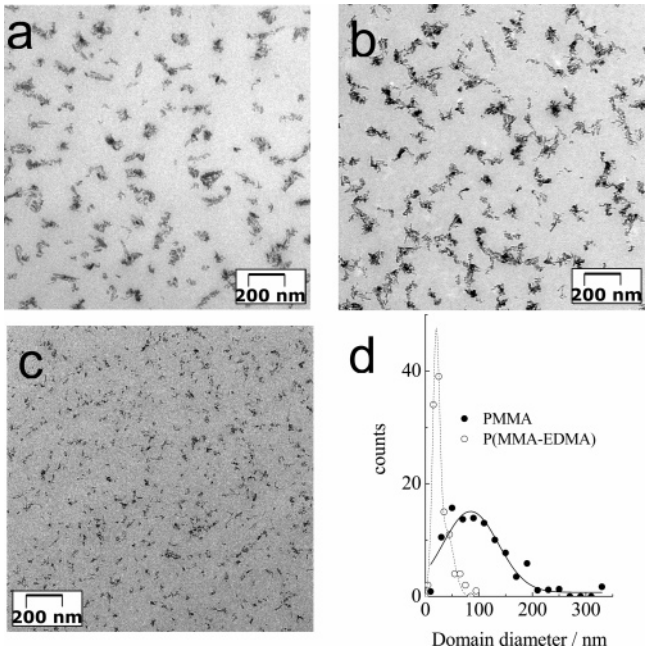

Figure 8. TEM images of ZnO nanoparticles in (a) linear PMMA obtained by bulk polymerization using 1.5 wt % of AIBN, (b) linear PMMA obtained using 0.4 wt % AIBN, and (c) cross-linked poly(MMA−EDMA) copolymer obtained using 0.4 wt % AIBN. (d) Size distributions of ZnO clusters in linear PMMA from (a) and cross-linked poly(MMA−EDMA) from (c); data obtained by statistical treatment of TEM images.

was added, while the amount of particles, which induce transfer, was kept the same. No significant change in the kinetics of polymerization was thus expected and formed.

In contrast to linear polymer matrix, the cross-linked system is rigid and hinders the particles to meet each other by diffusion. Figure 8c presents the particles in a cross-linked polymer matrix which was obtained in the presence of 0.25% mol of EDMA with respect to MMA. After 3 h polymerization, the system was a network which did not dissolve in tetrahydrofuran or acetone even after 3 days. The cross-linking points are formed around the particles which are homogeneously distributed initially in the monomer, and they may be confined in meshes of the polymer network knitted by branching and cross-linking centers. The size of chains in between these centers may be comparable with the particle diameter because at the same polymerization conditions without using EDMA, R_h of the formed polymers was measured at 11 nm. ZnO particles appear as almost nonaggregated in TEM micrograph (Figure 8c). The size distribution of ZnO domains in the cross-linked PMMA shifts to smaller diameters and becomes comparable with the distribution obtained in the monomer (compare Figures 8d and 6a). Consequently, the architecture of the polymer chains, but not size, makes a clear difference in the dispersion of tBuPO$_3$H$_2$-coated ZnO nanoparticles in the polymer matrix.

Small-angle X-ray scattering (SAXS) can be useful to evaluate the average dispersion of nanoscale additives in polymer matrix. Although a full scale and detailed investigations of SAXS of these samples goes beyond the intention of this report, we can, nevertheless, gain qualitative insights. The scattering power of the samples presented in Figure 8a,c was examined by SAXS. Figure 9 shows scattering intensities of these two samples as a function of scattering vector, q. A strong decay with increasing magnitude of q is seen in both cases. Although both of the samples contain the same amount of ZnO, the composite prepared with linear PMMA shows higher intensity as compared to the one prepared with cross-linked P(MMA−EDMA). It is necessary to mention that the measurements were performed using an incident beam which provides the same power and probes the same scattering volume, i.e., the same thickness of films, within the same illumination time. The intensity of scattering is known to be proportional to the

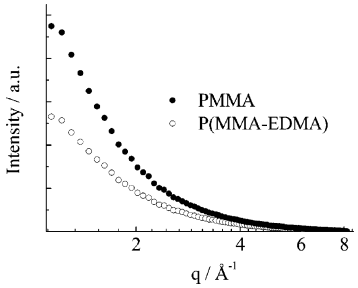

Figure 9. SAXS spectra of the composites that contain the same amount of ZnO dispersed into linear PMMA and cross-linked P(MMA−EDMA).

contrast $(\rho_{ZnO} - \rho_{PMMA})^2$ in electron densities of the scatterers and the matrix, to the number of scattering elements in the irradiated volume, N_{domain}, and to the volume of individual scatterers, V^2_{domain}. Thus, the intensity can be written[51,52]

$$I(q) \propto (\rho_{ZnO} - \rho_{PMMA})^2 N_{domain} V^2_{domain} \quad (5)$$

This expression allows the comparison of samples differing in the level of particle dispersion. In the present case one needs to recall the information obtained from the TEM images as follows: (i) In the sample presented in Figure 8a, about six individual particles are assumed to pack into an octahedron-shaped cluster in which the voids between the densely packed spherical particles is filled with matrix polymer.[53] Each of the clusters is considered as one scattering element. A sharp increase in electron density at the interface between the ZnO domains and polymer matrix depleted from the particles causes a strong contrast for the probing X-ray beam. In a first approximation, the contrast in electron densities of the scatters and the medium was expressed by the difference in bulk densities of the "ZnO cluster" and PMMA. The density of these clusters was calculated following a simple mixing rule, and not surprisingly, it appeared to be lower than that of the naked ZnO particle itself. The average number of scattering elements, i.e., ZnO clusters, is taken as $N_1/6$. (ii) In the sample demonstrated in Figure 8c, the scattering volume consists of N_1 individual ZnO particles with an average diameter 22 nm. The contrast was estimated using the bulk densities of "ZnO" and the polymer since the particles are well dispersed in P(MMA−EDMA) without clustering or packing. As a result of the calculation, scattering of the former composite was found to have higher intensity as compared to the latter one. This result is consistent with our SAXS measurements. However, the experimental value gave smaller difference in scattering intensities than the estimated one. In fact, the samples described above were assumed to behave in an ideal manner which may not be the case. For example, in the first case, the assumption of hexagonal packing may not hold for the whole population of the particles; i.e., not all of the particles may be involved in formation of clusters, and the cluster may have a size distribution. Another reason for rigorous agreement could be the contribution of branching and cross-linking points which act as additional scattering centers in the latter case, and they reduce the difference between the scattering intensities (Figure 8c). In short, the results of SAXS certainly support the idea that the dispersion of particles in the branched and cross-linked matrix is more homogeneous.

A homogeneous dispersion is enabled by holding the particles in a matrix in which the network formation is faster than the segregation of particles. The onset of the gelation process is very difficult to predict in this system for several reasons: (i) the kinetics of polymerization is complex including copolymerization of EDMA as well as transfer, (ii) the onset determined in the literature depends strongly on the technique used to measure it, and (iii) the gelation process does not occur homogeneously. Furthermore, premature gelation at the wall of the reactor has been observed and attributed to surface effects,[54] which may play a very important role in this work. The formation of cross-linking points around the particles, if it happens in this system, could be a reason why better particle dispersion was obtained.

Scheme 1. Cartoon Demonstrating the Architecture of PMMA Matrices and Their Effect on the State of Dispersion of Nanoparticles: (a) Depletion Interparticle Attraction Causes Aggregation of Nanoparticles That Are Surrounded by Chains Smaller than the Diameter of Nanoparticles; (b) Dispersion of Individual Nanoparticles Being Encapsulated in a Cross-Linked Polymer Cage Larger Than a Particle (the Depletion Is Kinetically Hindered)

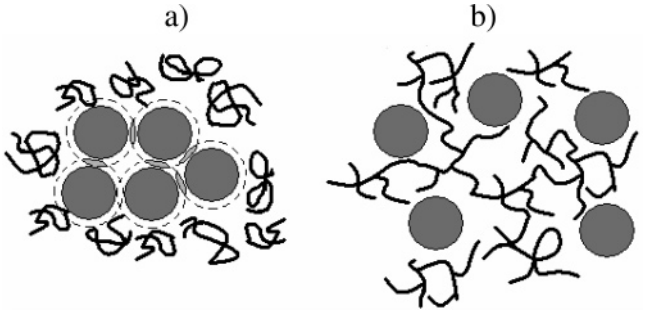

The arrangements of the particles with linear and cross-linked PMMA are graphically illustrated in Scheme 1. As described in a related reference,[19] in linear chains, on the left panel, the center of polymer molecules is excluded from coming closer than a certain distance to the surface of colloids because of high entropic cost of configurational distortion. Each colloid is therefore surrounded by a depletion zone (dotted circle) within which there is essentially no polymer center of mass. If the surfaces of two colloids are closer than twice the size of the depletion zone, then there is no polymer in the lens-shaped region (shaded), and a net osmotic force presses the particles together—the depletion attraction. Upon incorporation of a difunctional comonomer into a homogeneous dispersion (on the right panel) where particles are individually dispersed, the system undergoes cross-linking without giving sufficient time for diffusion and segregation of nanoparticles, resulting in a stable particle dispersion.

In addition to the architecture of polymeric molecules obtained in situ, there are several experimental parameters need to be examined for future work as suggested by recent theoretical and computational studies.[55,56] Decreasing of particle size smaller than 22 nm (∼5−10 nm) diameter will be important since the magnitude of oscillatory depletion interparticle forces scales with particle-to-monomer ratio. Smaller forces may reduce the aggregation tendency of particles. Other parameters to improve the quality of particle dispersion in polymers may be strength of monomer−particle and direct interparticle attractions. In the present case, the particles were hydrophobized by treatment with alkylphosphonic acids. We claim that the systems are athermal where particle−polymer attraction is minimum.[23] The work can be extended using hydrophobic surfactants having available vinyl groups that can join the polymerization in bulk. Thereby, polymer chains are grafted to the particle surface, and the particle−polymer interaction is increased in contrast to the present system. Surfactants with different alkyl and functional groups may provide various ranges

of monomer−particle and interparticle attractions that may have strong influence on the quality of particle dispersion.

Conclusion

PMMA-based composites with nanoparticles of oxides and nitride were produced via free radical polymerization of homogeneous monomer/particle dispersions. The particles markedly improve both the free radical polymerization process and the microstructure of the in-situ-formed PMMA chains. The autoacceleration is suppressed, resulting in a better control of heat dissipation and MWDs. In contrast to common belief the particles to be dispersed are not neutral components but have considerable and important reactivity and therefore interfere with the mechanism of polymerization. Chemisorbed water and oxygen on the particles surface, which are considered as reactive impurities, may react with propagating free radicals. The reaction proposed in this article is degenerative transfer of hydrogen atoms abstracted from the surface-adsorbed water. This transfer reaction improves the thermal stability of polymer chains by reducing the amount of weak linkages and end groups. Nanoparticles segregate during the formation of linear PMMA chains most probably because of depletion attraction which is a general drawback of in-situ polymerization. The homogeneity of particle dispersion is enhanced by the in-situ copolymerization of MMA with a difunctional monomer. The formation of three-dimensional network by cross-linking reduces the tendency of segregation of the nanoparticles upon polymerization.

Acknowledgment. The authors thank R. Munoz-Espí for his help at the initial stages of the experiments and Prof. Veith of INM at Saarbrücken for providing the ZrO_2 nanoparticles.

References and Notes

(1) Balazs, A. C.; Emrick, T.; Russell, T. P. *Science* **2006**, *314*, 1107−1110.
(2) Beecroft, L. L.; Ober, C. K. *Chem. Mater.* **1997**, *9*, 1302−1317.
(3) Kickelbick, G. *Prog. Polym. Sci.* **2003**, *28*, 83−114.
(4) Nagao, M.; Kumashiro, R.; Matsuda, T.; Kuroda, Y. *Thermochim. Acta* **1995**, *253*, 221−233.
(5) Highfield, J. G.; Bowen, P. *Anal. Chem.* **1989**, *61*, 2399−2402.
(6) Henderson, M. A. *Surf. Sci. Rep.* **2002**, *46*, 5−308.
(7) Li, Y. Q.; Qiu, T.; Xu, J. *Mater. Res. Bull.* **1997**, *32*, 1173−1179.
(8) Nosaka, A. Y.; Nosaka, Y. *Bull. Chem. Soc. Jpn.* **2005**, *78*, 1595−1607.
(9) Clark, J. W.; Hall, P. G.; Pidduck, A. J.; Wright, C. J. *J. Chem. Soc., Faraday Trans. 1* **1985**, *81*, 2067−2082.
(10) Linsebigler, A. L.; Lu, G. Q.; Yates, J. T. *Chem. Rev.* **1995**, *95*, 735−758.
(11) Matsuno, R.; Yamamoto, K.; Otsuka, H.; Takahara, A. *Chem. Mater.* **2003**, *15*, 3−5.
(12) Jethmalani, J. M.; Sunkara, H. B.; Ford, W. T.; Willoughby, S. L.; Ackerson, B. J. *Langmuir* **1997**, *13*, 2633−2639.
(13) Advincula, R.; Zhou, Q. G.; Park, M.; Wang, S. G.; Mays, J.; Sakellariou, G.; Pispas, S.; Hadjichristidis, N. *Langmuir* **2002**, *18*, 8672−8684.
(14) Carrot, G.; Diamanti, S.; Manuszak, M.; Charleux, B.; Vairon, I. P. *J. Polym. Sci., Polym. Chem.* **2001**, *39*, 4294−4301.
(15) Advincula, R. C. *J. Dispersion Sci. Technol.* **2003**, *24*, 343−361.
(16) Zhu, J. J.; van Ommen, J. G.; Lefferts, L. *Catal. Today* **2006**, *117*, 163−167.
(17) Hoffman, A. J.; Yee, H.; Mills, G.; Hoffmann, M. R. *J. Phys. Chem.* **1992**, *96*, 5540−5546.
(18) Krauetler, B.; Reiche, H.; Bard, A. J. *J. Polym. Sci., Polym. Lett. Ed.* **1979**, *17*, 535.
(19) Poon, W. C. K. *J. Phys.: Condens. Matter* **2002**, *14*, R859−R880.
(20) Piech, M.; Weronski, P.; Xu, X.; Walz, J. Y. *J. Colloid Interface Sci.* **2002**, *247*, 327−341.
(21) Lecerf, N.; Mathur, S.; Shen, H.; Veith, M.; Hufner, S. *Scr. Mater.* **2001**, *44*, 2157−2160.
(22) Demir, M. M.; Espi-Munoz, R.; Lieberwirth, L.; Wegner, G. *J. Mater. Chem.* **2006**, *16*, 2940−2947.
(23) Demir, M. M.; Koynov, K.; Akbey, Ü.; Bubeck, C.; Park, I.; Lieberwirth, I.; Wegner, G. *Macromolecules* **2007**, *40*, 1089−1100.
(24) Demir, M. M.; Memesa, M.; Castignolles, P.; Wegner, G. *Macromol. Rapid Commun.* **2006**, *27*, 763−770.
(25) Public domain software to be downloaded from http://rsb.info.nih.gov/ij/ (National Institute of Health).
(26) Balke, S. T.; Hamielec, A. E. *J. Appl. Polym. Sci.* **1973**, *17*, 905.
(27) Trommdorff, E. H. K.; Lagally, P. *Macromol. Chem.* **1948**, *1*, 169.
(28) Buback, M.; Egorov, M.; Gilbert, R. G.; Kaminsky, V.; Olaj, O. F.; Russell, G. T.; Vana, P.; Zifferer, G. *Macromol. Chem. Phys.* **2002**, *203*, 2570−2582.
(29) Dixon, K. W. In *Polymer Handbook*, 4th ed.; Brandgup, J., Immergut, E. H., Grulke, E. A., Eds.; J. Wiley & Sons: New York, 1999; p II/1.
(30) Ignatchenko, A.; Nealon, D. G.; Dushane, R.; Humphries, K. *J. Mol. Catal. A: Chem.* **2006**, *256*, 57−74.
(31) Lisachenca, A.; Vilesov, F. I. *Sov. Phys. Tech. Phys.* **1969**, *14*, 442-&.
(32) Solomon, D. H. *J. Macromol. Sci., Chem.* **1982**, *A17*, 337−367.
(33) Kashiwagi, T.; Inaba, A.; Brown, J. E.; Hatada, K.; Kitayama, T.; Masuda, E. *Macromolecules* **1986**, *19*, 2160−2168.
(34) Allock, H. R.; Lampe, F. W. *Contemporary Polymer Chemistry*, 2nd ed.; Prentice Hall: Englewood Cliffs, NJ, 1981.
(35) Grassie, N.; Melville, H. W. *Proc. R. Soc. London A* **1949**, *199*, 39−55.
(36) Kashiwagi, T.; Morgan, A. B.; Antonucci, J. M.; VanLandingham, M. R.; Harris, R. H.; Awad, W. H.; Shields, J. R. *J. Appl. Polym. Sci.* **2003**, *89*, 2072−2078.
(37) Smith, G. B.; Russell, G. T. *Macromol. Symp.*, submitted for publication.
(38) Bhattach, B.; Nandi, U. *J. Polym. Sci., Part A: Polym. Chem.* **1966**, *4*, 2675.
(39) Nandi, U. S.; Palit, S. R.; Ghosh, P. *Nature (London)* **1962**, *195*, 1197.
(40) De Bruyn, H.; Gilbert, R. G.; Hawkett, B. S. *Polymer* **2000**, *41*, 8633−8639.
(41) Lee, T. Y.; Guymon, C. A.; Jonsson, E. S.; Hoyle, C. E. *Polymer* **2004**, *45*, 6155−6162.
(42) Moad, G.; Solomon, D. H. In *The Chemistry of Radical Polymerization*; Elsevier: Amsterdam, 2006; pp 279−331.
(43) Wight, F. R. *J. Polym. Sci., Part C: Polym. Lett.* **1978**, *16*, 121−127.
(44) Flory, P. J. *Principles of Polymer Chemistry*; Cornell University Press: Ithaca, NY, 1953; Vol. VII.
(45) Raghavan, R.; Maver, T. L.; Blum, F. D. *Macromolecules* **1987**, *20*, 814−818.
(46) Moussaid, A.; Poon, W. C. K.; Pusey, P. N.; Soliva, M. F. *Phys. Rev. Lett.* **1999**, *82*, 225−228.
(47) Aranguren, M. I.; Mora, E.; Macosko, C. W. *J. Colloid Interface Sci.* **1997**, *195*, 329−337.
(48) Mackay, M. E.; Tuteja, A.; Duxbury, P. M.; Hawker, C. J.; Van Horn, B.; Guan, Z. B.; Chen, G. H.; Krishnan, R. S. *Science* **2006**, *311*, 1740−1743.
(49) Walling, C. *J. Am. Chem. Soc.* **1945**, *67*, 441−447.
(50) Landin, D. T.; Macosko, C. W. *Macromolecules* **1988**, *21*, 846−851.
(51) Peterlik, H.; Fratzl, P. *Mon. Chem.* **2006**, *137*, 529−543.
(52) Alexander, L. E. In *X-Ray Diffraction Methods in Polymer Science*; Burke, E., Chalmers, B., Krumhansl, J. A., Eds.; Wiley-interscience: New York, 1969; p 286.
(53) Manoharan, V. N.; Elsesser, M. T.; Pine, D. J. *Science* **2003**, *301*, 483−487.
(54) Whitney, R. S.; Burchard, W. *Macromol. Chem. Phys.* **1980**, *181*, 869−890.
(55) Hooper, J. B.; Schweizer, K. S. *Macromolecules* **2005**, *38*, 8858−8869.
(56) Hooper, J. B.; Schweizer, K. S. *Macromolecules* **2006**, *39*, 5133−5142.

MA070142E